

Monte Carlo simulation of an Ising antiferromagnet with competing Glauber and Kawasaki dynamics

B. C. S. Grandi and W. Figueiredo

Departamento de Física, Universidade Federal de Santa Catarina, 88040-900 Florianópolis, Santa Catarina, Brazil

(Received 16 June 1997)

In this work we consider a two-dimensional antiferromagnetic Ising model in contact with a heat bath at temperature T , and subject to an external source of energy. The dynamics of this model is governed by the competition between two stochastic processes: the Glauber dynamics with probability p , which simulates the contact with the heat bath, and the Kawasaki one with probability $1-p$, which takes into account the flux of energy into the system. By employing Monte Carlo simulations, we have found the phase diagram for the stationary states of the system, as well as the corresponding critical exponents. The phase diagram is very similar to the one obtained through dynamical pair approximation. Conversely to the ferromagnetic case, this Ising antiferromagnet does not exhibit the phenomenon of self-organization. [S1063-651X(97)05011-3]

PACS number(s): 64.60.Ht

I. INTRODUCTION

In a previous paper [1] we found a stationary phase diagram of the two-dimensional Ising antiferromagnet when the system is subject to two independent competing stochastic dynamics: the one-spin-flip Glauber dynamics [2], with probability p , and the two-spin-exchange Kawasaki dynamics [3], with probability $1-p$. The role of these two dynamics concerning the symmetries of the system is quite different: the Glauber kinetics always changes the order parameter, while the Kawasaki one conserves the ferromagnetic order parameter but not the antiferromagnetic order parameter. We can think about this system as being coupled to a heat bath at a given temperature, and subject to an external flux of energy. The contact with the heat reservoir can be simulated by the Glauber process, while the input of energy into the system can be associated with the Kawasaki process. By employing the dynamical pair approximation, we showed that this system exhibits only the antiferromagnetic and the paramagnetic stationary states. For values of $p \leq 0.968$, this competing Ising antiferromagnet presents only the paramagnetic phase. That is, the antiferromagnetic state is easily destroyed by a very small flux of energy into the system. Then the phase diagram of this model in the plane temperature versus probability p shows a continuous transition line, which separates the stationary antiferromagnetic and paramagnetic phases.

The behavior of the ferromagnetic version of this competing model was studied by Tomé and de Oliveira [4] in the dynamical pair approximation. They showed that this system exhibits the interesting phenomenon of self-organization: the system goes continuously from a ferromagnetic to a paramagnetic state as we increase the flux of energy into the system. By increasing this flux more and more, it is possible to pass from the disordered paramagnetic to an ordered antiferromagnetic phase. On the other hand, Grandi and Figueiredo [5] have performed Monte Carlo simulations for this model in a square lattice. The phase diagram obtained from simulations is completely different from the one determined by the dynamical pair approximation: although it ap-

pears a very small antiferromagnetic region in the phase diagram, that is, only for $p \leq 0.073$, and, at very high temperatures, we note that, at very small temperatures, the only stable phase is the ferromagnetic one, and the phenomenon of self-organization disappears in the limit of zero temperature.

In this work we study the antiferromagnetic Ising model in two dimensions with competing Glauber and Kawasaki kinetics, as described above. We employ extensive Monte Carlo simulations and finite-size analysis in order to find the phase diagram and the critical exponents of the model. As the results of simulations in the ferromagnetic case changed significantly the picture of self-organization, we wonder if similar simulations performed in the antiferromagnetic version of the model could furnish a different diagram from that found in the dynamical pair approximation analysis.

II. DYNAMICS OF THE MODEL

Here we consider an antiferromagnetic Ising model on a square lattice with N lattice sites. The state of the system is represented by $\sigma = (\sigma_1, \sigma_2, \dots, \sigma_N)$, where the spin variable assumes the values $\sigma_i = \pm 1$. The energy of the system in the state σ is given by

$$E(\sigma) = J \sum_{(i,j)} \sigma_i \sigma_j, \quad (1)$$

where the summation is only over nearest-neighboring spins and $J > 0$. Let $P(\sigma, t)$ be the probability of finding the system in the state σ at time t . The evolution of $P(\sigma, t)$ is given by the following master equation:

$$\frac{dP(\sigma, t)}{dt} = \sum_{\sigma'} [P(\sigma', t)W(\sigma', \sigma) - P(\sigma, t)W(\sigma, \sigma')], \quad (2)$$

where $W(\sigma', \sigma)$ gives the probability, per unit time, for the transition from the state σ' to state σ . We assume that the two competing processes can be written as

$$W(\sigma', \sigma) = pW_G(\sigma', \sigma) + (1-p)W_K(\sigma', \sigma), \quad (3)$$

where

$$W_G(\sigma', \sigma) = \sum_{i=1}^N \delta_{\sigma'_1, \sigma_1} \delta_{\sigma'_2, \sigma_2} \cdots \delta_{\sigma'_i, -\sigma_i} \cdots \delta_{\sigma'_N, \sigma_N} w_i(\sigma) \quad (4)$$

and

$$W_K(\sigma', \sigma) = \sum_{(i,j)} \delta_{\sigma'_1, \sigma_1} \delta_{\sigma'_2, \sigma_2} \cdots \delta_{\sigma'_i, \sigma_j} \cdots \delta_{\sigma'_j, \sigma_i} \cdots \delta_{\sigma'_N, \sigma_N} \times w_{ij}(\sigma), \quad (5)$$

where in the above summation only pairs of nearest-neighbors spins are considered.

In these equations, $W_G(\sigma', \sigma)$ is the one-spin flip Glauber process, which simulates the contact with the heat bath at temperature T , and $W_K(\sigma', \sigma)$ is the two-spin flip, which simulates the flux of energy into the system. Also, $w_i(\sigma)$ is the transition probability of flipping spin i , while $w_{ij}(\sigma)$ is the transition probability of exchanging two nearest-neighbors spins i and j .

The contact with the heat bath at temperature T is given by the following prescription:

$$w_i(\sigma) = \min \left[1, \exp \left(- \frac{\Delta E_i}{k_B T} \right) \right], \quad (6)$$

where ΔE_i is the change in energy when spin i is flipped.

On the other hand, for the two-spin-exchange Kawasaki dynamics, we take the following expression for $w_{ij}(\sigma)$:

$$w_{ij}(\sigma) = \begin{cases} 0 & \text{for } \Delta E_{ij} \leq 0 \\ 1 & \text{for } \Delta E_{ij} > 0 \end{cases} \quad (7)$$

where ΔE_{ij} is the energy after the exchange of the neighboring spins i and j minus the energy before the exchange.

III. MONTE CARLO SIMULATIONS

We have considered Monte Carlo simulations on a square lattice with $L \times L = N$ sites, with the values of L ranging from $L=4$ up to 64. We have taken periodic boundary conditions in all of our simulations. We considered different initial conditions in order to guarantee that the final stationary states we use in our calculations are the correct ones.

We follow the steps described below to find the stationary states of the system as a function of p and T : for selected values of the probability p and temperature T , we choose at random a spin i , from a given initial configuration. Then we generate a random number ξ_1 between zero and unity. If $\xi_1 \leq p$, we choose to perform the Glauber process; in this case we calculate the value of $w_i(\sigma)$ and generate another random number ξ_2 . If $\xi_2 \leq w_i(\sigma)$, we flip spin i , otherwise do not. If $\xi_1 > p$ we go over the Kawasaki process. We again generate another random number ξ_3 in order to select one of the four nearest-neighbors of the spin i , say j . Then we find the value of w_{ij} and we exchange the selected spins only if $w_{ij} = 1$. We have discarded the first $10^4 N$ Monte Carlo steps in order to attain the stationary regime, for all lattice sizes we consider. One Monte Carlo step equals N single-spin flips or an exchange of spins trials. In order to estimate the quantities of interest, we used 5×10^4 Monte Carlo steps to calculate the averages for any lattice size.

We can evaluate the stationary phase diagram of the model and its associated critical exponents by using the finite-size scaling concepts [6] applied to some thermodynamic properties of the system. For a system with linear dimension L , we define, at the stationary states, the reduced staggered magnetization M_L , susceptibility χ_L , and the fourth-order cumulant [7] U_L by the following expressions:

$$M_L = \langle |m| \rangle, \quad (8)$$

$$\chi_L = N \{ \langle m^2 \rangle - \langle |m| \rangle^2 \}, \quad (9)$$

$$U_L = 1 - \frac{\langle m^4 \rangle}{3 \langle m^2 \rangle^2}, \quad (10)$$

where $m = (1/N) \sum_{i=1}^N \sigma_i$.

These above defined quantities obey the following finite-size scaling relations in the neighborhood of the stationary critical point T_c :

$$M_L(T) = L^{-\beta/\nu} M_0(L^{1/\nu} \epsilon), \quad (11)$$

$$\chi_L(T) = L^{\gamma/\nu} \chi_0(L^{1/\nu} \epsilon), \quad (12)$$

$$U_L(T) = U_0(L^{1/\nu} \epsilon), \quad (13)$$

where $\epsilon = T - T_c$.

If we derive Eq. (13) with respect to the temperature T , we obtain the scaling relation

$$U'_L(T) = L^{1/\nu} U'_0(L^{1/\nu} \epsilon), \quad (14)$$

so that $U'_L(T_c) = L^{1/\nu} U'_0(0)$. Then we can find the critical exponent ν from the log-log plot of $U'_L(T_c)$ versus L .

IV. PHASE DIAGRAM AND CRITICAL EXPONENTS

The critical temperature for every value of p can be determined approximately by a plot of the staggered magnetization M_L as a function of $1/L$ for different values of temperature T . For instance, in Fig. 1 we exhibit this kind of plot for the selected value $p=0.99$ and for values of T in the range $1.6 \leq T \leq 2.2$: it is easy to see that the magnetization changes abruptly between the values $T=1.9$ and 2.0 , in units of J/k_B . For values of $T \leq 1.9$ the magnetization is almost constant for all values of L , which characterizes an ordered stationary antiferromagnetic state. On the other hand, for values of $T \geq 2.0$, the staggered magnetization, while remaining finite for any value of L , decreases as $1/L$ for each value of T .

In order to locate better the critical temperature T_c of the model, in Fig. 2 we plot, for $p=0.99$, the reduced fourth-order cumulant $U_L(T)$, defined by Eq. (10), as a function of temperature T , for several values of L as indicated in the figure. The scaling relation for the fourth-order cumulant shows that, at the critical temperature, all curves of $U_L(T)$ must intercept themselves at T_c for whatever value of L . From the latter figure we estimate the value of T_c as being 1.92 ± 0.01 . We considered other values of p in our analysis in order to determine the complete phase diagram of the model. In Fig. 3 we exhibit the phase diagram we obtain in the plane $\eta = \exp(-J/k_B T)$ versus $1-p$. As we can see, the

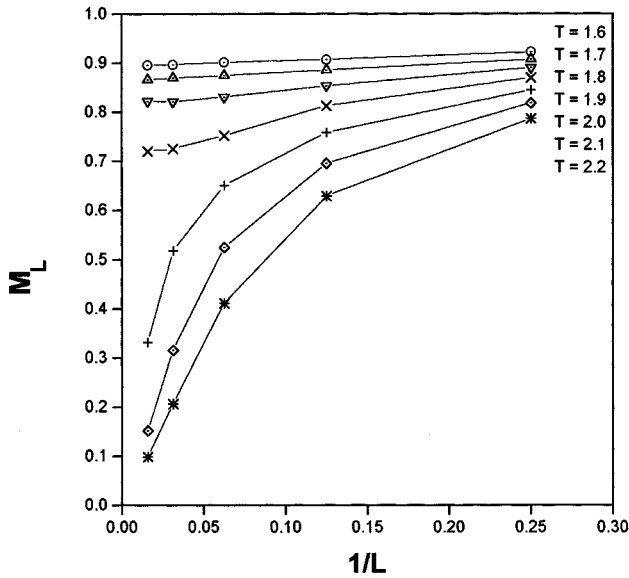


FIG. 1. Staggered magnetization M_L as a function of $1/L$ for several values of T and $p=0.99$. The transition appears for $1.9 \leq T \leq 2.0$.

antiferromagnetic phase occupies a very small region of the phase diagram. As $1-p$ gives the probability of occurrence of Kawasaki dynamics, then the nonequilibrium antiferromagnetic states are destroyed by a small flux of energy into the system. At $T=0$, the critical value of p is 0.965; surprisingly, the value we determined in our simulations is the same as we have found in the dynamical pair approximation [1], that is, $p_c=0.968$. Again, we have shown that this competing antiferromagnetic Ising model does not present the self-organization phenomenon. As opposed to the ferromagnetic case, where results from the dynamical pair approximation

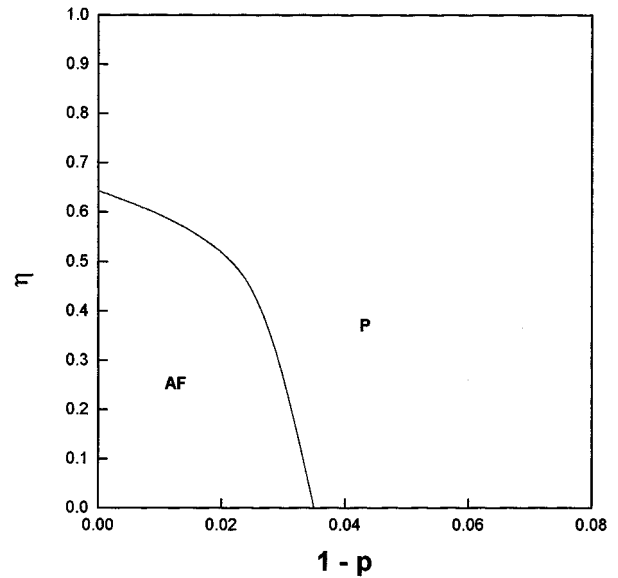


FIG. 3. Phase diagram of the two-dimensional competing anti-ferromagnetic Ising model. $\eta = \exp(-J/k_B T)$ and $1-p$ is related to the flux of energy. *AF* and *P* refer to antiferromagnetic and paramagnetic phases, respectively.

and Monte Carlo simulations were quite different, here, for the corresponding antiferromagnetic model, both calculations gave very closely results concerning the phase diagram.

From our Monte Carlo simulations, we can also evaluate the critical exponents of the model. From Eq. (14) we see that, at the critical temperature T_c , $U'_L(T_c)$ scales as $L^{1/\nu}$. Then, from the log-log plot of $U'_L(T_c)$ versus L , as can be seen in Fig. 4, for $p=0.99$, the best fit to the Monte Carlo data gives us $\nu=1.00 \pm 0.04$.

In Fig. 5 we exhibit the log-log plot of the staggered magnetization, at the critical temperature T_c , $M_L(T_c)$ versus L , for $p=0.99$. From the slope of the straight line, which is

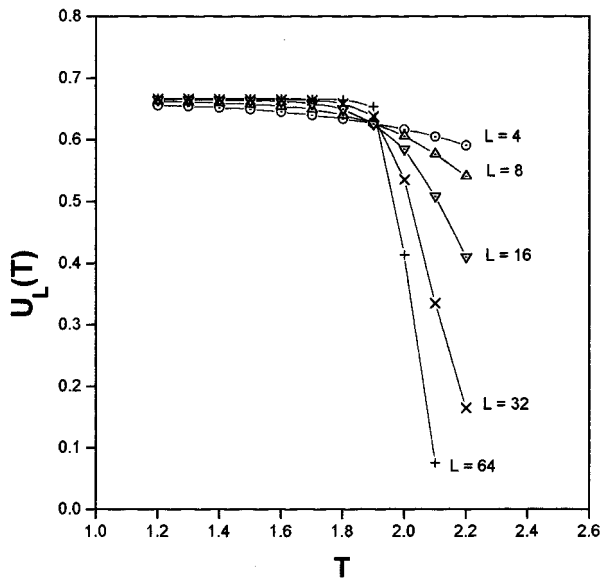


FIG. 2. Reduced fourth-order cumulant $U_L(T)$ as a function of temperature T for several values of the lattice size L and $p=0.99$. The broken lines serve as a guide to the eyes. The critical temperature is $T_c = 1.92 \pm 0.01$.

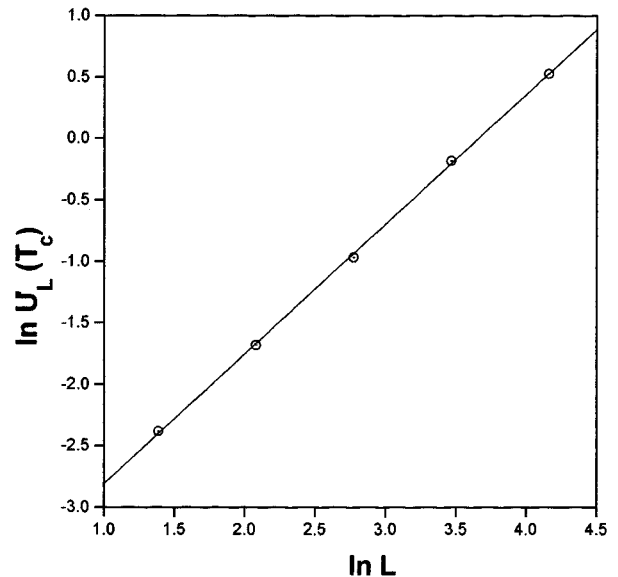


FIG. 4. Log-log plot of $U'_L(T_c)$ vs L for $p=0.99$. The straight line is the best fit to the data, which gives $\nu=1.00 \pm 0.04$.

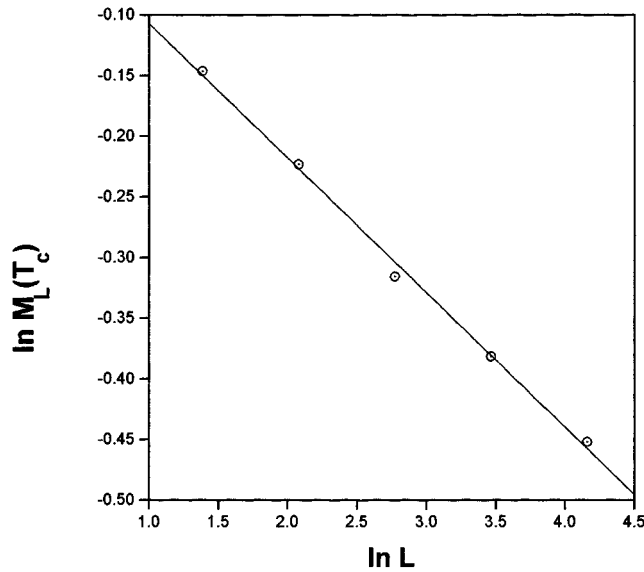


FIG. 5. Log-log plot of the magnetization $M_L(T_c)$ vs L for $p = 0.99$. From the slope of the straight line, which is the best fit to the data points, we obtain $\beta/\nu = 0.11 \pm 0.01$.

the best fit to the data points, and using Eq. (11), we can obtain the value of the stationary critical ratio β/ν . Then, our estimate is $\beta/\nu = 0.11 \pm 0.01$.

Another stationary critical exponent of interest is that associated with the susceptibility. We can find the value of the ratio γ/ν by employing two different approaches based on the scale relation given by Eq. (12). In the first case we can construct a log-log plot of $\chi_L(T)$ versus L , at the stationary critical temperature T_c ; then, from the slope of the straight line, which is the best fit to the data points, we can obtain, for $p = 0.99$, the value $\gamma/\nu = 1.72 \pm 0.02$, as can be seen in

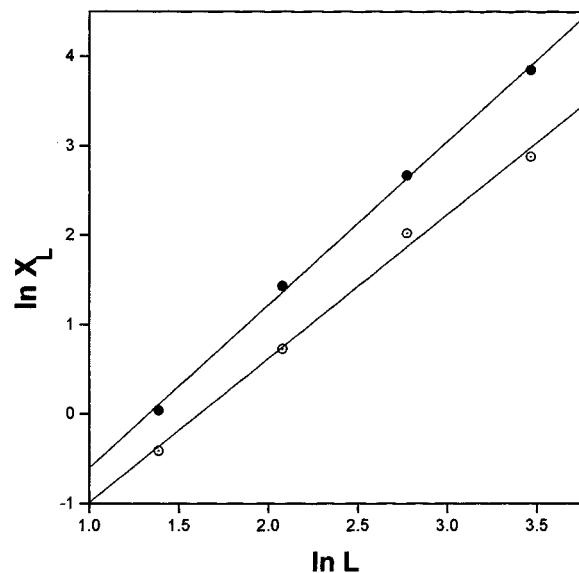


FIG. 6. Log-log plots of the susceptibility $\chi_L(T)$ vs L . Open circles mean $\chi_L(T)$ at $T = T_c$, and solid circles mean $\chi_L(T)$ at its maximum. The straight lines are the best fits to the data points. From these slopes we obtain open circles, $\gamma/\nu = 1.72 \pm 0.02$, and solid circles, $\gamma/\nu = 1.74 \pm 0.01$.

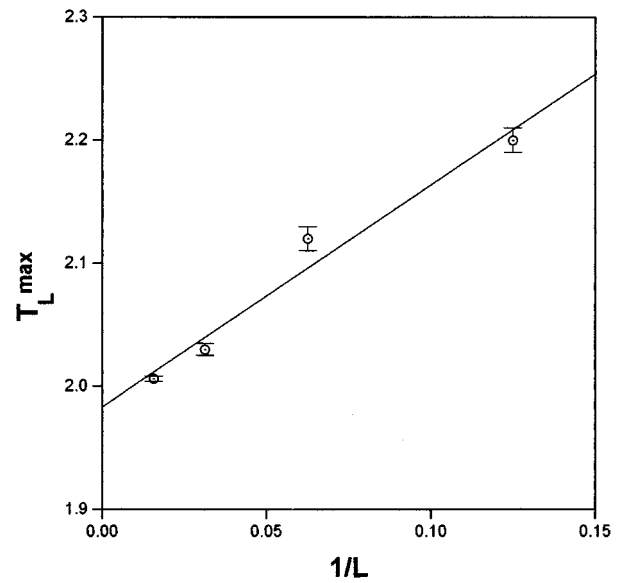


FIG. 7. Behavior of T_L^{\max} , the value of T at which the susceptibility is maximum, vs $1/L$. The extrapolated value as $L \rightarrow \infty$ is $T^{\max} = 1.95$.

Fig. 6. We can also estimate the same ratio by a log-log plot of the maximum value of the susceptibility versus L . It is easy to see that if T_L^{\max} is the value of T for which $\chi_L(T)$ is maximum, then $T_L^{\max} = T_c + (u^{\max}/L^{1/\nu})$, where u^{\max} is a constant independent of L which maximizes $\chi_0(u)$. Based on these arguments, we immediately see that the maximum of the susceptibility also scales as $L^{\gamma/\nu}$. In this way, from Fig. 6, the value we obtain for this ratio is $\gamma/\nu = 1.74 \pm 0.01$, at $p = 0.99$. As to be expected, the value of T_L^{\max} goes to the value of T_c when L becomes very large. Therefore, in Fig. 7,

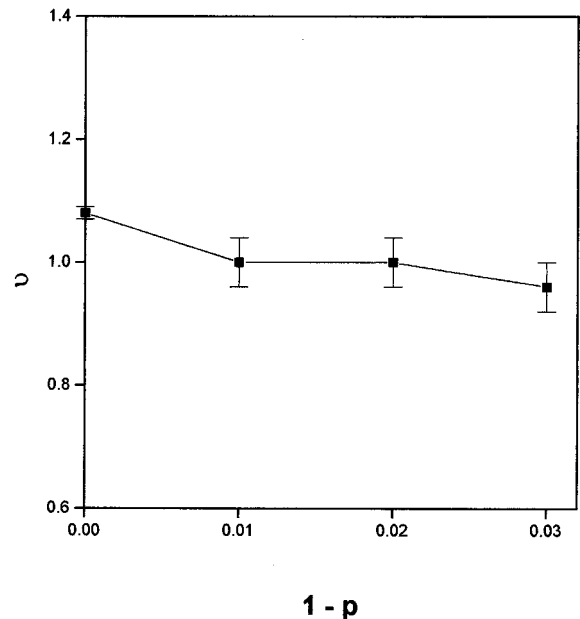


FIG. 8. Critical exponent ν as a function of $1 - p$ at the critical line represented in Fig. 3. The error bars give the accuracy of our Monte Carlo data points. The estimated values of ν are around the corresponding exact equilibrium value $\nu = 1$.

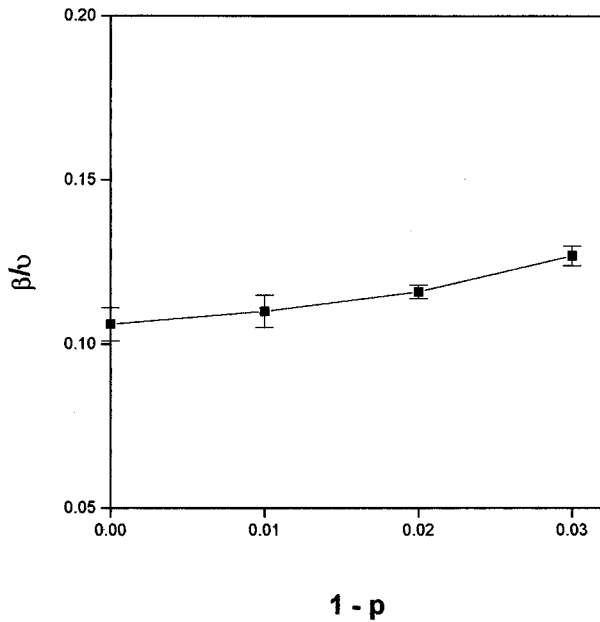


FIG. 9. Ratio β/ν as a function of $1-p$ at the critical line transition. The estimated values of this ratio oscillate around the exact equilibrium value $\frac{1}{8}$.

we show the plot of T_L^{\max} as a function of the inverse of lattice size. From the extrapolation of the straight line, which is the best fit to the data, we find that $T_c = 1.95 \pm 0.03$.

In Figs. (8–10) we exhibit the plots we obtained for ν , β/ν , and γ/ν , respectively, for other values of the competition parameter at the stationary critical line of the phase diagram of Fig. 3. We would like to stress that the values we have obtained for these critical exponents compare very well with the analogous static exponents of the corresponding two-dimensional equilibrium Ising model. As our nonequilibrium model preserves the up-down symmetry, it is expected that it belongs to the same universality class of the equilibrium Ising model [8,9]. In a recent review, Schmittmann and Zia [10] discussed general arguments about universality classes on driven diffusive systems which evolve to nonequilibrium steady states.

V. CONCLUSION

We have determined the phase diagram and studied the stationary critical properties of a nonequilibrium antiferro-

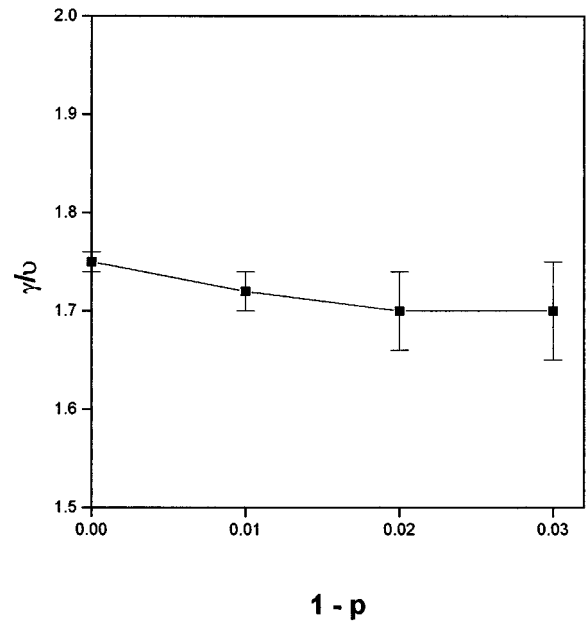


FIG. 10. Ratio γ/ν as a function of $1-p$ at the transition line between antiferromagnetic and paramagnetic stationary phases. Within the accuracy of our data points, the values of this ratio oscillate around the exact equilibrium value $\frac{7}{4}$.

magnetic Ising model in a square lattice, where the system is in contact with a heat bath at temperature T , and subject to an external flux of energy. The exchange of energy with the heat reservoir is assumed to be represented by the stochastic Glauber process, while the flux of energy into the system is simulated by a kind of Kawasaki diffusive process. The phase diagram of the model we have obtained through Monte Carlo simulations is quite similar to that found in the dynamical pair approximation, and confirms that this model does not exhibit the self-organization phenomenon. We have also calculated the critical exponents associated to this model, and we have found that its values are in accordance with those of the corresponding equilibrium Ising model in two dimensions.

ACKNOWLEDGMENT

This work was partially supported by the Brazilian agencies CNPq and FINEP.

-
- [1] B. C. S. Grandi and W. Figueiredo, *Phys. Rev. B* **50**, 12 595 (1994).
 [2] R. J. Glauber, *J. Math. Phys.* **4**, 294 (1963).
 [3] K. Kawasaki, in *Phase Transitions and Critical Phenomena*, edited by C. Domb and M. S. Green (Academic, London, 1972), Vol. 4.
 [4] T. Tomé and M. J. de Oliveira, *Phys. Rev. A* **40**, 6643 (1989).
 [5] B. C. S. Grandi and W. Figueiredo, *Phys. Rev. E* **53**, 5484 (1996).
 [6] V. Privman, *Finite-Size Scaling and Numerical Simulation of*

- Statistical Systems* (World Scientific, Singapore, 1990).
 [7] K. Binder, *Z. Phys. B* **43**, 119 (1981).
 [8] G. Grinstein, C. Jayaparakash, and Yu He, *Phys. Rev. Lett.* **55**, 2527 (1985).
 [9] K. E. Bassler and B. Schmittmann, *Phys. Rev. Lett.* **73**, 3343 (1994).
 [10] B. Schmittmann and R. K. P. Zia, in *Phase Transitions and Critical Phenomena*, edited by C. Domb and J. L. Lebowitz (Academic, New York, 1997).